Homologous-targeting biomimetic nanoparticles co-loaded with melittin and a photosensitizer for the combination therapy of triple negative breast cancer

Tao Zhang[a,b,1], Liya Bai[a,1], Ran You[a], Meng Yang[a], Qian Chen[a], Yuanyuan Cheng[a], Zhanyin Qian[a], Yinsong Wang[a,*] and Yuanyuan Liu[a,*]

[a] *Key Laboratory of Immune Microenvironment and Disease (Ministry of Education), The Province and Ministry Co-sponsored Collaborative Innovation Center for Medical Epigenetics, Tianjin Key Laboratory on Technologies Enabling Development of Clinical Therapeutics and Diagnostics (Theranostics), School of Pharmacy; Department of Genetics, School of Basic Medical Sciences, Tianjin Medical University, Tianjin 300070, China*

[b] *Department of Pharmacy, Tianjin First Central Hospital, Tianjin 300192, China*

[1] These two authors contributed equally to this work.

* Corresponding authors

E-mail addresses: liuyuanyuan01@tmu.edu.cn (Y. Liu), wangyinsong@tmu.edu.cn (Y. Wang)

Materials and methods

Materials

Monoclonal antibodies against CD11c-PE, CD62L-APC, and CD44-PE were provided by eBioscience (San Diego, CA, USA). Monoclonal antibodies against CD80-FITC, CD86-APC, and Rabbit anti-CD31 polyclonal antibody were obtained from Abcam (Cambridge, UK). Monoclonal antibodies against Ki67, CD8, and Alexa-Fluor 647-labeled goat anti-rabbit secondary antibodies were purchased from Invitrogen (Carlsbad, NM, USA). Rabbit anti-HMGB1 antibody and Rabbit anti-calreticulin/AF488 antibody were provided by Biosynthesis Biotechnology (Beijing, China). Singlet oxygen sensor green (SOSG), LIVE/DEAD cell imaging kit, Annexin-V-FITC/PI cell apoptosis kit, Coomassie brilliant blue methylthiazolyldiphenyl-tetrazolium bromide (MTT), hematoxylin & eosin (H&E) and TNF-α, IFN-γ ELISA kit were bought from Meilun Biotech (Dalian, China).

Cellular uptake and homologous tumor targeting ability of MDM@TPP nanoparticles *in vitro*

The specific uptake of the MDM@TPP nanoparticles was assessed by confocal microscopy and flow cytometry. Briefly, the HUVECs, Hepa1-6 cells and 4T1 cells were seeded into 12-well plates equipped with glass coverslips and then were incubated with TPP nanoparticles or MDM@TPP nanoparticles for 4 h. Afterward, these cells were stained with DAPI and observed under a confocal microscope. Moreover, the fluorescence intensity of intracellular mTHPC was detected by flow cytometry.

Penetration of MDM@TPP nanoparticles into tumor spheroids

According to the previous reported method, we constructed 3D tumor cell spheroids and then cultured them with MDM@TPP nanoparticles. After incubation for 6 h and 12 h, the

fluorescence localization of mTHPC in the tumor spheroids was observed and photographed using a confocal microscope.

Live/dead cell staining and cell apoptosis assay

To visually observe the cytotoxicity of the above treatments, the cells were evaluated by live/dead cell staining. Briefly, 4T1 cells were seeded in 12-well plates at a density of 6×10^4 cells per well and incubated for 24 h. Then, the cells were cultured with mTHPC, TPP nanoparticles or MDM@TPP nanoparticles. In the NIR laser irradiation groups, the cells were exposed to a 652 nm laser and then cultured for an additional 24 h. After processing with the reagents of the LIVE/DEAD cell staining kit, the cells were observed under a confocal microscope.

4T1 cells were seeded into 12-well plates at a density of 8×10^4 cells per well and cultured for 24 h. The cells were then incubated with Mel, MDM, mTHPC, TPP nanoparticles or MDM@TPP nanoparticles. In the NIR laser irradiation groups, the cells were exposed to a 652 nm laser. After incubation for another 24 h, the collected cells were stained with the reagents of an Annexin-V-FITC/PI apoptosis kit and analyzed using a flow cytometer.

ICD effect of MDM@TPP nanoparticles

The exposure of calreticulin (CRT) was analyzed in 4T1 cells using FACS analysis and immunofluorescence staining. In brief, 4T1 cells were incubated with therapeutic agents and irradiated with a laser as described above. Then, the cells were stained with anti-calreticulin/AF488 antibody (1:200) for 40 min, analyzed with a flow cytometer and imaged with a confocal microscope. The intracellular release of HMGB1 was detected by

immunofluorescence staining. After receiving various treatments, the cells were separately incubated with a primary rabbit anti-HMGB1 polyclonal antibody overnight at 4 °C, followed by processing with a secondary FITC-labeled goat anti-rabbit antibody. Finally, the cells were stained with DAPI and observed under a confocal microscope.

***In vitro* evaluation of bone marrow-derived dendritic cells (BMDCs) maturation**

BMDCs were collected from normal female BALB/c mice bone marrow and cultured according to the previous method. First, 4T1 cells were inoculated in 12-well plates and treated with mTHPC, Mel, MDM, TPP nanoparticles or MDM@TPP nanoparticles. The cells were partially given the laser irradiation and cultured for an additional 24 h. Next, the antigen-containing supernatant from each well was collected and added to BMDCs inoculated in 12-well plates. After incubation for 24 h, the cells were costained with anti-CD80-FITC and anti-CD86-APC antibodies. Finally, the expression levels of the costimulatory molecules CD80 and CD86 were determined by flow cytometry.

***In vivo* biodistribution and PDT efficacy study**

The biodistribution and TNBC targeting ability of MDM@TPP nanoparticles was assessed in 4T1 tumor-bearing mice using a fluorescence imaging system (PerkinElmer, Waltham, USA). The mice were injected with the normal saline (the control), mTHPC, TPP nanoparticles or MDM@TPP nanoparticles via the tail vein. At 6 h, 12 h, 24 h and 48 h after administration, the mice were sacrificed, and their main organs and tumors were observed by a fluorescence imaging system.

We further evaluated the PDT efficacies of mTHPC, TPP nanoparticles and MDM@TPP nanoparticles combined with laser irradiation in 4T1 tumor-bearing mice using

the singlet oxygen probe SOSG. Twenty hours after injection of therapeutic agents, the mice were injected intratumorally with 50 μL of 50 μM SOSG and subsequently received laser irradiation at the tumor site. The mice were sacrificed to collect the tumors, and the intensity of green fluorescence was observed by fluorescence microscopy.

Evaluation of the synergistic antitumor effects *in vivo*

Bilateral tumor models were established on both sides of the backs of mice back as primary and distal tumors 7 d and 1 d before treatment, respectively. When the 4T1-Luc primary tumors grew to approximately 60 mm^3, the mice were randomly divided into 8 groups with 10 mice in each group. Normal saline (control), MDM, mTHPC, TPP nanoparticles or MDM@TPP nanoparticles were injected intravenously. At 24 h after administration, the primary tumors of the mice in the NIR laser irradiation group were treated with 652 nm laser irradiation. The mice were further treated with radiation twice a day for 7 consecutive days during the entire treatment period, and the volumes of both the primary and distal tumors and body weights were recorded every 2 d.

We collected the main organs of the mice in each group at the end of treatment and observed 4T1 cell metastasis with a luminescence imaging system. Furthermore, sections of these tissues were stained with H&E. The primary tumor sections were processed separately with antibodies against Ki67 and CD31. Based on the manufacturer's protocols, the cells were then stained with HRP-linked secondary antibody. These stained tissue sections were observed by microscopy. To evaluate memory antitumor immunity, spleens selected from 3 mice were digested to obtain single-cell suspensions. These cells were stained with anti-CD62L-APC and anti-CD44-PE antibodies and detected by flow cytometry.

In addition, immunofluorescence and ELISA analyses of serum were used to analyze the extent of immune activation in the treated mice 48 h after the first therapeutic agents were combined with laser irradiation. Three mice selected randomly from each group were sacrificed 2 d after one treatment, and their tumors, spleens and blood samples were collected for the following examinations. Specifically, we ground and digested the collected spleen tissues to obtain single-cell suspensions. Then, these cells were separately coincubated with anti-CD3-FITC, anti-CD4-PE and anti-CD8-APC antibodies according to the manufacturers' protocols. Finally, all stained cells were analyzed using a flow cytometer. We further analyzed the secretion levels of IFN-γ and TNF-α in the serum of the abovementioned mice with ELISA kits.

Figures

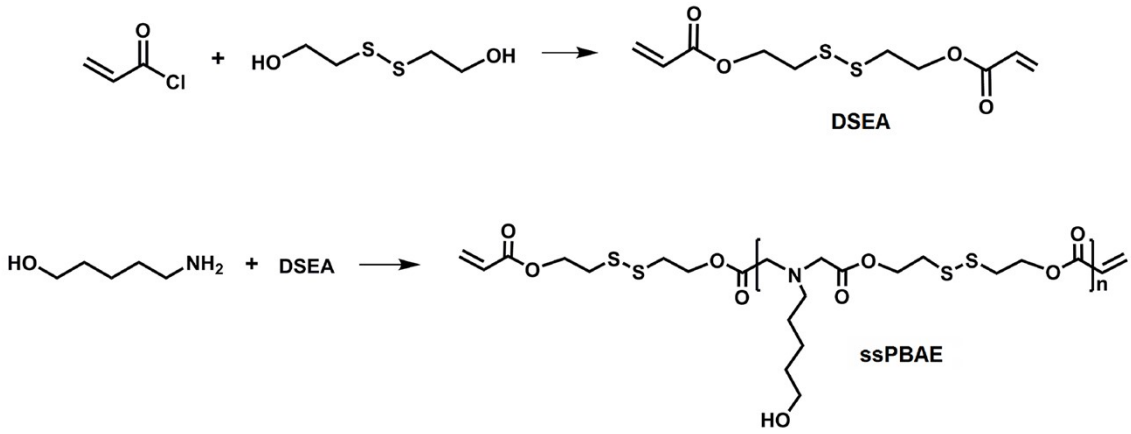

Figure S1. Illustration for the synthesis route of ssPBAE.

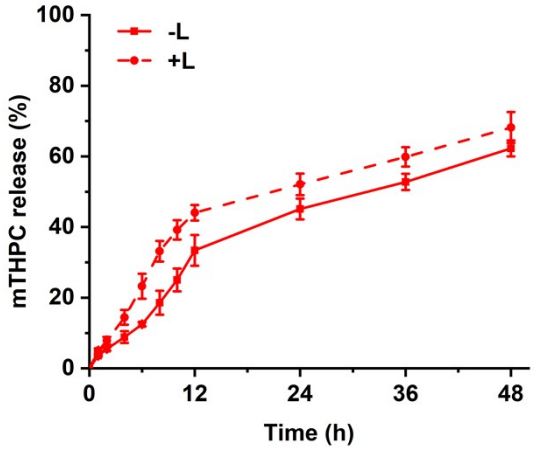

Figure S2. The *in vitro* release of mTHPC from MDM@TPP nanoparticles at PBS solution with pH value 7.4 with or without laser irradiation.

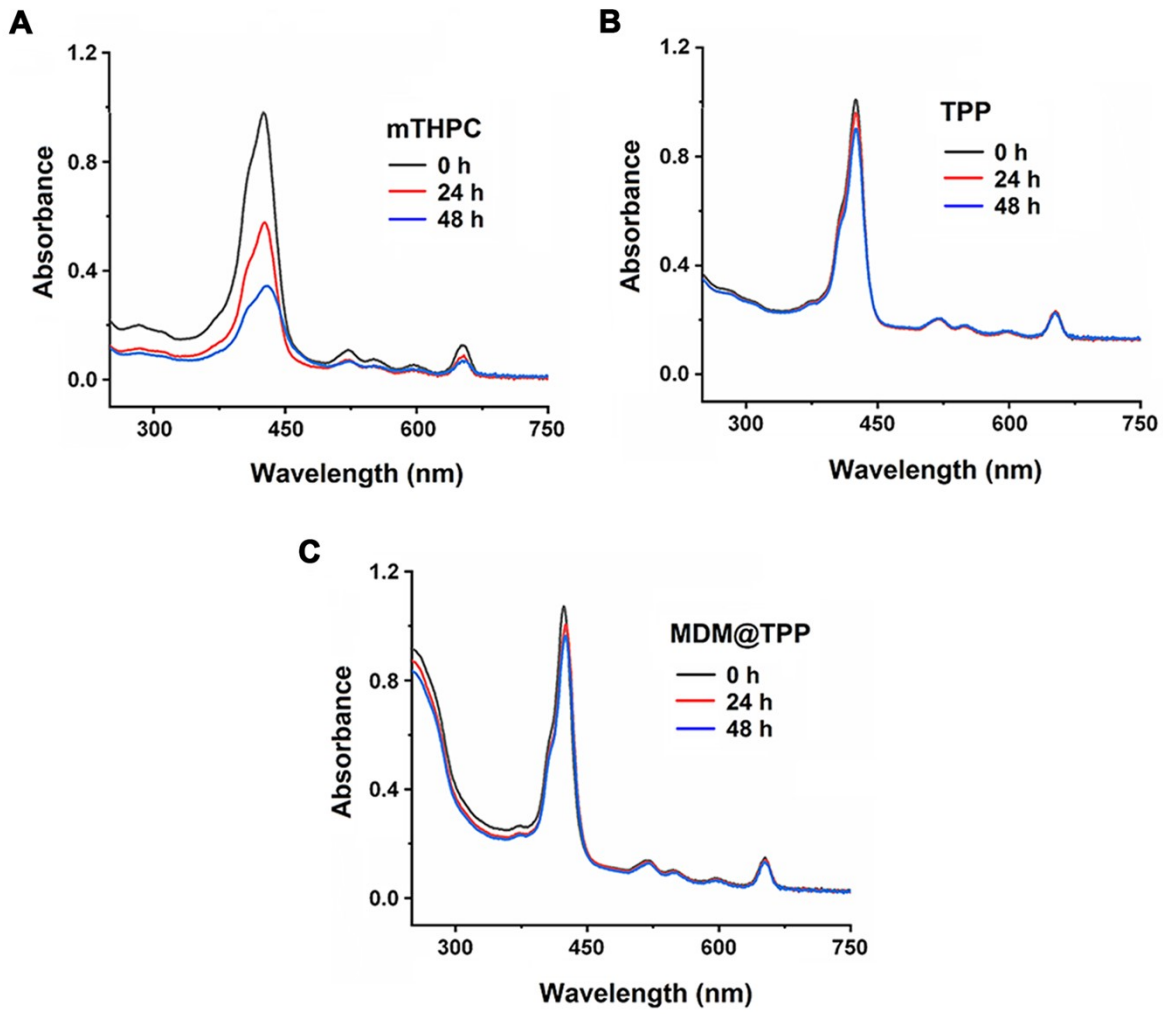

Figure S3. The UV spectra changes of mTHPC (A), TPP nanoparticles (B) and MDM@TPP nanoparticles (C) during 48 h storage.

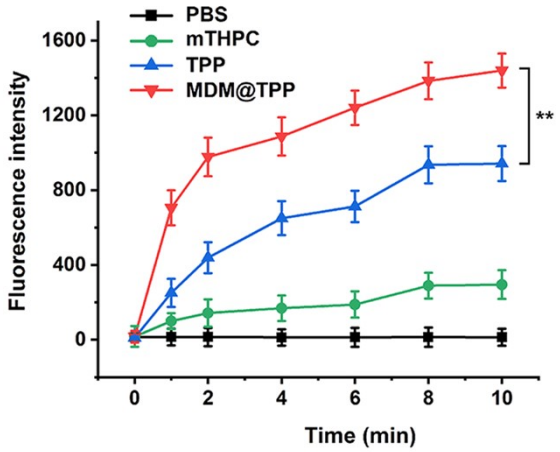

Figure S4. The ROS generation of PBS, mTHPC, TPP nanoparticles and MDM@TPP nanoparticles after laser irradiation (*n=3*). ** represents comparison between two groups $P < 0.01$.

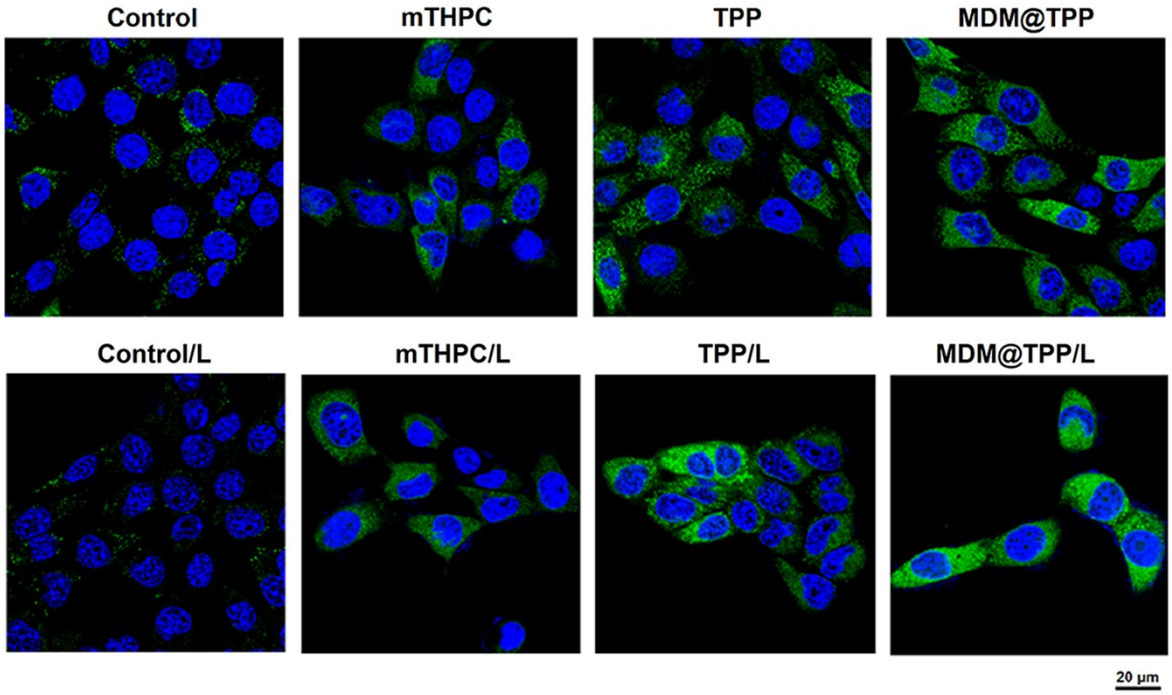

Figure S5. The confocal microscopic images of 4T1 cells treated with free mTHPC, TPP nanoparticles and MDM@TPP nanoparticles alone and with laser irradiation. Rhodamine 123 was used as a probe for detecting the mitochondrial membrane potentials with green fluorescence.

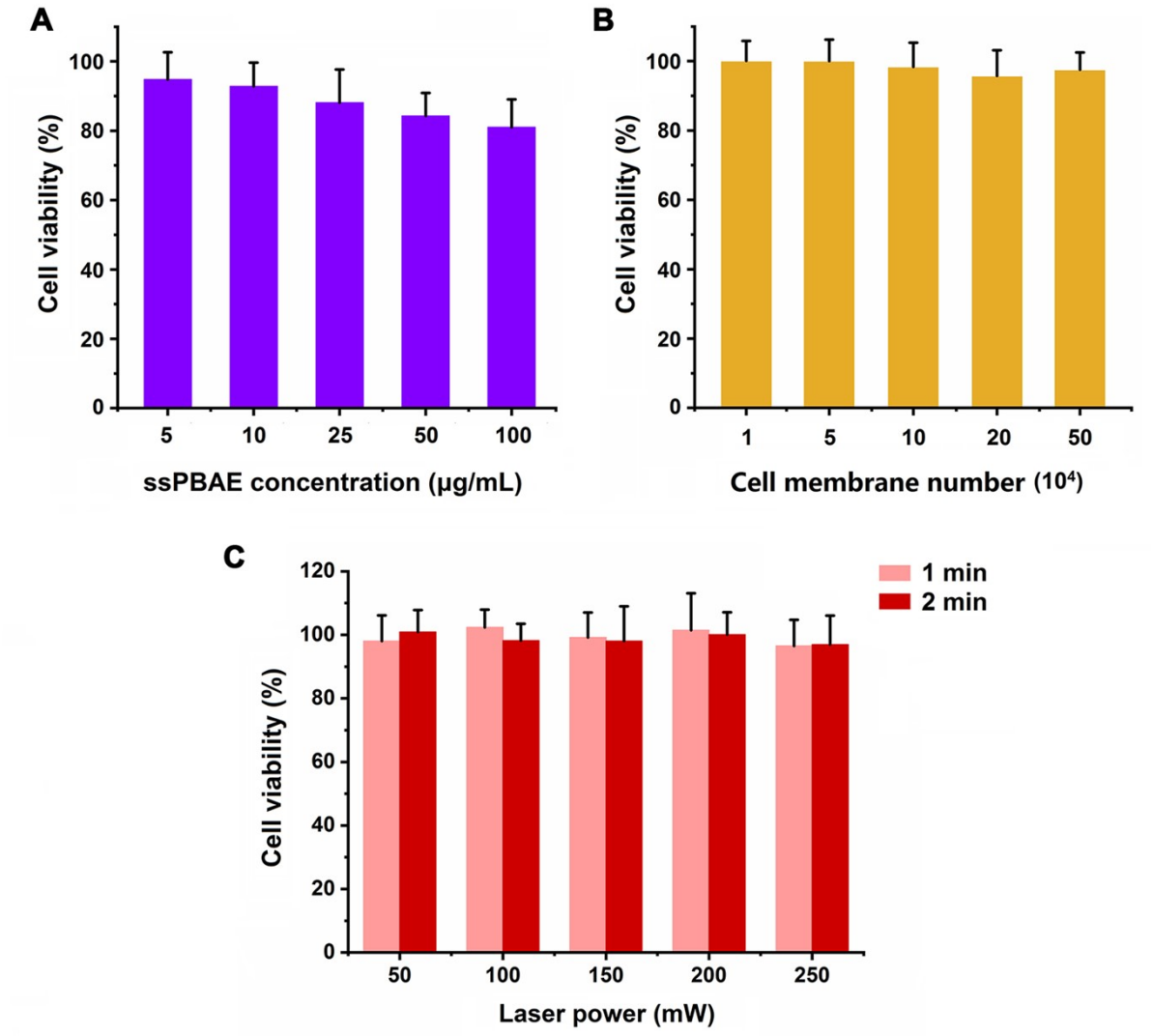

Figure S6. Influence of carrier materials and laser irradiation on the growth of 4T1 cells *in vitro*. The cytotoxicity of PLGA/ssPBAE nanoparticles (A) and different amounts of tumor cell membrane (B) co-incubated with 4T1 cells for 24 h. (C) Survival of 4T1 cells 24 h after irradiation.

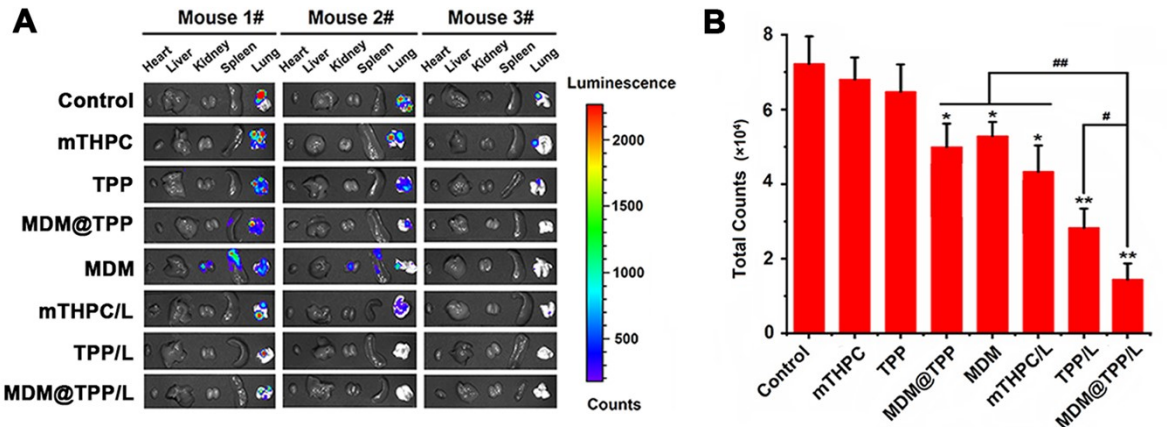

Figure S7. Bioluminescence images of tumor metastasis on main organs (heart, liver, spleen, lung and kidney) of mice (A) and luminescence intensity of lung metastases (B) in each treatment group ($n=3$). * and ** represents comparison with control group $P < 0.05$ and $P < 0.01$. # and ## represents comparison between two groups $P < 0.05$ and $P < 0.01$.

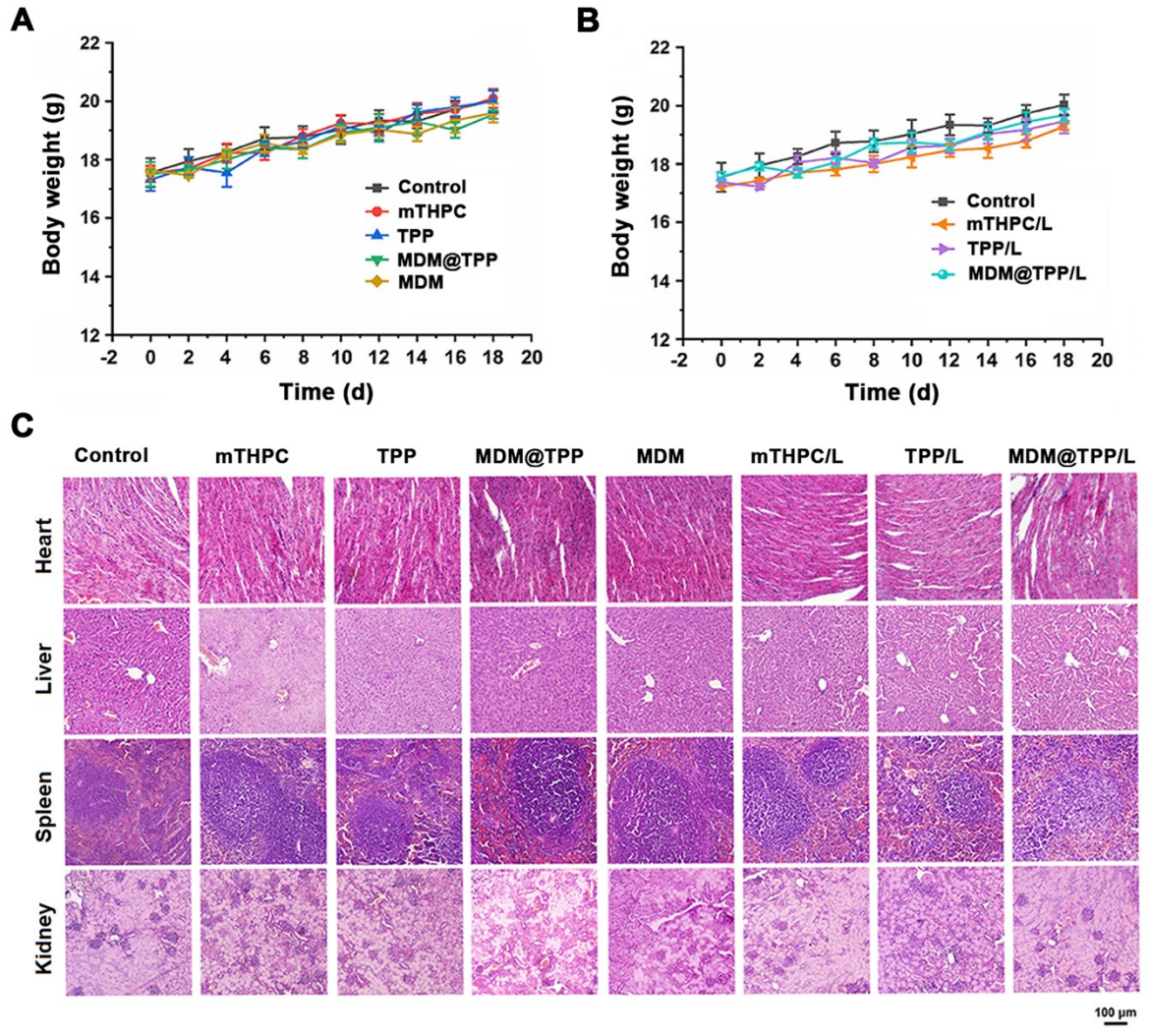

Figure S8. The body weight change curves (A, B) of tumor-bearing mice during treatment.

(C) The H&E staining microscopic images of main organs (heart, liver, spleen and kidney) of mice after treatment.

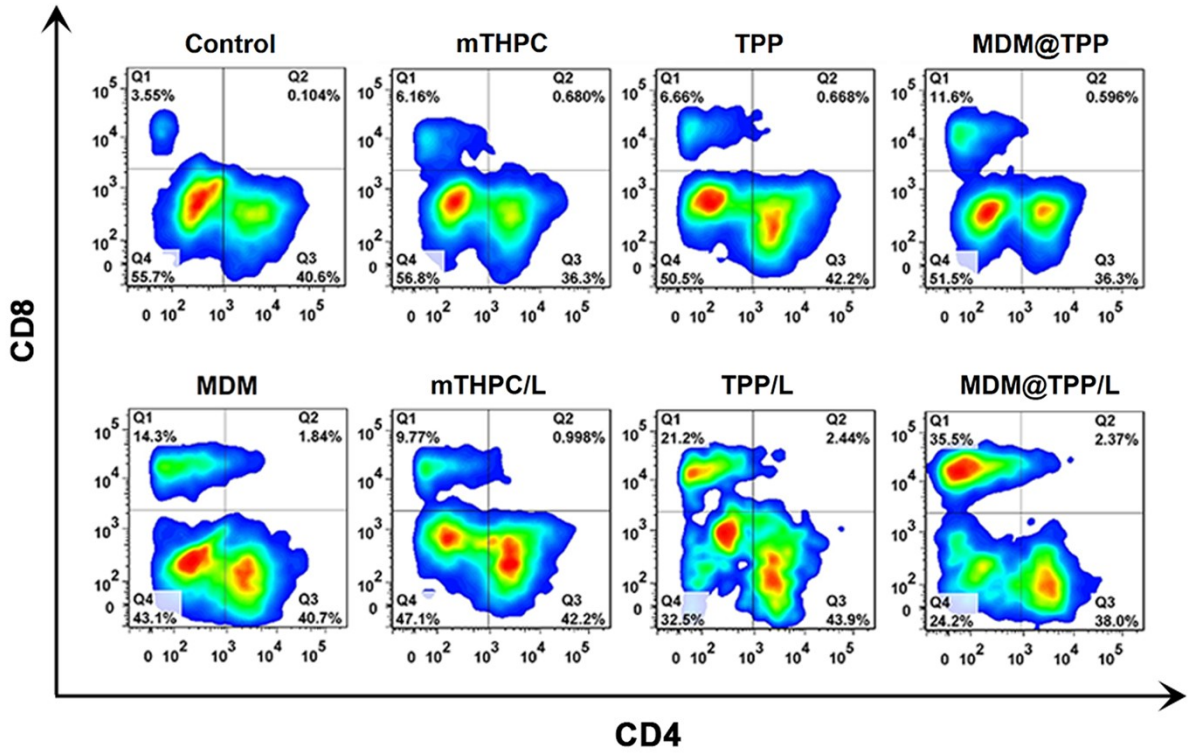

Figure S9. Flow cytometry analysis of $CD4^+$ T lymphocytes and $CD8^+$ T lymphocytes of primary tumors in each treatment group.